Spontaneous and Self-Assembled Line Formations on Silicon Substrates with Vanadium Pentoxide Sol−Gels

Craig Calvert, Kelly A. Burke, and Steven L. Suib*

Department of Chemistry, Unit 3060, 55 North Eagleville Road, University of Connecticut, Storrs, Connecticut 06269-3060

Received: May 6, 2005; In Final Form: October 3, 2005

A simple one-pot method has been developed to deposit discreet nanometer line formations on silicon substrates without any surface pretreatment starting with vanadium pentoxide sol−gels. These vanadium suspensions were made by hydrolyzing amorphous V_2O_5 in water. The properties of the vanadium clusters were determined through X-ray diffraction, elemental analyses, pH calculations, and concentration calculations. Morphology of the lines was examined with optical microscopy, atomic force microcoscopy, and scanning electron microscopy. Infrared spectroscopy was used to inspect the organic components. The vanadium sol−gel used formed discreet and regular lines with high reproducibility and on the same order of magnitude as other patterning techniques. Previous research with a low solubility, 8 g/L, metal oxide for line, ring, or helix formation has not been found in the literature; this work could lead to novel applications of metal oxides such as porous catalysts, battery materials, and resistive electronic materials.

Introduction

Vanadium and manganese oxide sol−gel chemistry has received a great deal of interest in materials synthesis. These materials are used in many applications including batteries,[1] nanowire arrays,[2] nanoribbons,[3] and porous catalysts.[4] Inorganic helices of porous manganese oxides have recently been prepared.[5] A standard microscope slide was placed in a beaker with the manganese oxide sol−gel inside. The system was heated until the water evaporated; left on the slides were lines. Helices were formed when this system was confined. The initial experiments have led to further studies[6] and a proposed mechanism[7] for the formation of these spontaneous and self-assembled inorganic structures. Line formations such as these have been made with a number of processes. Natural line formation processes are spontaneous. The most studied natural processes are Liesegang Rings which were discovered in the early 1900s.[8] Studies have also been done on the formation of line patterns formed on silicon wafers by a drying water film.[9] Current synthesis methods are different than the natural processes because they are not spontaneous[10,11] or they require considerable time.[12] The most widely used method for line synthesis is photolithography, which is used to manufacture circuit boards. Etching done either physically or chemically is used to form precise patterns.[13] Another method involves templating, which uses a mold and forces compounds into the mold that is then removed.[10]

Vanadium pentoxide gels have been known since 1885, when Ditte[14] mixed ammonium vanadate and nitric acid. With the recent focus on sol−gel processes, interest in vanadium gels has escalated. Vanadium pentoxide materials are common catalysts[15−18] due to mobile lattice oxygens, the inherent electronic structure and properties, and the physical shape of the crystal.[19−21] Careful control of reaction parameters along with varying the substrate could enhance relevant properties depending on the use of the designated material.

Sol−gel chemistry often involves the use of Al or Si. The versatility of these materials allows them to be used for ceramic membranes,[22] coatings,[23,24] films,[24] and numerous other applications. With so much focus on the Al and Si based sol−gels, vanadium sol−gels have not been studied as extensively. Part of the reason could be the less stable nature of transition metal sols and gels. There are several ways to synthesize vanadium pentoxide sol−gel material. The most widely used process for industry involves pouring the molten oxide into water.[21] Other preparations start with the oxide followed by the addition of hydrogen peroxide[21] or hydration of the amorphous oxide.[21] A chemical reaction with ammonium vanadate and hydrochloric acid has produced gels.[21] Hydrolysis and hydrothermal treatment are two other methods of synthesis.[21] Interest has developed in using such materials as counter electrodes in electrochromic devices,[25] which has a promising future in the television screen industry.

The focus of this work is on combining the procedure and line-forming features of the previous manganese oxide line work in these labortaories[5,6] to form spontaneous self-assembled lines of vanadium on glass substrates. The vanadium oxide sol−gel was synthesized by the dissolution of the metal oxide in water. The procedure from previous work in this lab[5,6] was modified to produce a more straightforward method. Analysis was done with optical microscopy, atomic force microscopy, scanning electron microscopy, energy-dispersive X-ray analysis, and infrared spectroscopy. Line formations synthesized via this route with any metal oxide other than manganese have not been found in the current literature.

Methods

Synthesis. The suspensions were prepared by dissolving V_2O_5, Aldrich 99.6+%, in DDW (Doubly Distilled Water), pH 5.5. V_2O_5 was chosen for its properties and position in the

* Address correspondence to this author. Phone: (860)-486-2797. Fax: (860)-486-2981. E-mail: steven.suib@uconn.edu.

10.1021/jp052360k CCC: $30.25
Published on Web 10/29/2005

Periodic Table; previous research in this lab used only $KMnO_4$. Once the pH of the solution became stable, any undissolved metal compound was filtered and weighed to give an accurate molarity. To mimic the previous manganese work a 5% excess of tetramethylammonium bromide (TMABr), Acros 98%, was added to some solutions followed by the addition of butyl alcohol (2-butanol Sigma Aldrich 99%). Initial solutions were diluted to make lower concentrations. For calculation purposes 1 equiv of TMABr was added for every equivalent of metal atom.

After the solution was prepared, a glass microscope slide or silicon wafer was placed at a 60° angle in a beaker that contained the metal oxide solution; the electronics grade silicon wafers were obtained from a material science lab as pieces of larger broken wafers. Typically the slides and wafers were at room temperature before they were placed in the beaker. For some experiments glass slides were preheated in the oven at the temperature of the experiment before being placed in the beaker. The beaker containing the metal solution and wafer or slide was then placed in an oven until the water had evaporated completely. This was generally done overnight. There was no chemical pretreatment of the glass microscope slide; previous work has shown that no special preparations were necessary.[6]

Coating Procedure. A coating procedure was used to check the charge properties of the particles.[26] A quartz slide was cleaned with a solution of 30% H_2O_2, Fischer 30% in H_2O, and 70% H_2SO_4, J.T. Baker 93%, by volume and sonicated. Caution should be used when mixing peroxides and acids. After cleaning, the slide was dipped into alternating solutions of sodium poly(styrenesulfonate) (PSS) and poly(dimethyldiallylammonium) (PDDA) ending with the appropriate solution. Then the slides were placed into the vanadium solution and remained in the solution for one week. The slide was then removed and placed in a beaker with a mixture of nitric and hydrochloric acid to remove the coating. The solution was then diluted and analyzed with use of ICP.

Colloidal Silica Procedure. V_2O_5 solutions of concentrations 1.0×10^{-2}, 1.0×10^{-4}, 1.0×10^{-5}, and 1.0×10^{-6} M were added to solutions of colloidal silica, Aldrich Ludox HS-40 colloidal silica wt % in H_2O, with 40, 20, 5, 1, and 0.5 wt % of silica in an attempt to increase the amount of vanadium suspended by increasing the density of the solution. These solutions were then placed in the oven as stated above.

Characterization

Optical Microscopy. Images were acquired with an Olympus SZST base and lenses with a JVC TK-C1380 half inch CCD digital color camera and then stored on a computer as jpeg files.

Scanning Electron Microscopy (SEM)/Energy-Dispersive X-ray Analysis (EDAX). Scanning electron microscopy (SEM) and energy-dispersive X-ray (EDX) experiments were done to analyze surface and bulk elemental analyses, respectively. An Amray Model 1810 D SEM with a beam voltage of 20 kV with an Amray Model PV 9800 EDX system was used. Samples were calcined at 250 °C and mounted onto a sample holder for analysis.

Infrared Spectroscopy (IR). To gather data on the organic components, a Nicolet Magma-IR Spectrometer 750 with a nitrogen gas purge was used. Background was collected at the beginning of the runs and subtracted from the spectrum. Samples were prepared by mixing some of the desiccated material from several slides with KBr and pressed into a pellet. The spectrometer was then purged with nitrogen.

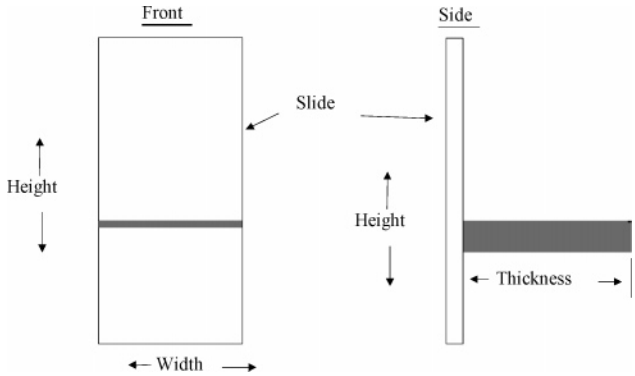

Figure 1. Diagram of terms used in the paper.

Atomic Force Microscopy (AFM). Tapping Mode Atomic Force Microscopy was used for topological analysis with a MultiMode scanning probe microscope with a stationary probe. Data were collected on a Nanoscope with version 4.x Digital Instruments software. A 50 nm carbon tip, with a 20 MHz peak rate, was used to a scan size of 50 μm and a scan rate of 0.1950 Hz, and the scan scale was set to 1.0000 μm. A total of 512 samples were done for each image.

X-ray Powder Diffraction (XRD). A Scintag Model PDS-2000 X-ray powder diffraction (XRD) was used to analyze crystallographic properties. The source was Cu Kα radiation at a power of 45 kV and a current of 40 mA. Sample scans were done at 5 deg/min. To prepare the samples microscope slides were laid horizontally in the oven and the metal oxide solution was deposited on them and left to evaporate. This was repeated until there was enough material built up to allow analysis. Calcination was done in air at 500 °C for 18 h.

Inductively Coupled Plasma (ICP). Further elemental analysis was performed with inductively coupled plasma-atomic emission spectroscopy (ICP-AES). A Perkin-Elmer 7-40 instrument equipped with an autosampler was used for the analyses at the Environmental Research Institute, Storrs, CT. Samples were dissolved in a mixed HCl and HNO_3 solution and then diluted with water.

Results

Synthesis. The equilibrium pH of the saturated V_2O_5 solution was around 3.5 with a concentration in the 10^{-3} range. When the pH was adjusted, the expected physical changes were visually observed.[21] The lines appeared similar even if neither the TMABr nor the butyl alcohol were used. The procedure from previous work[5,6] gave similar results to the one-pot procedure developed for this work. Heating the slides before putting them into the solution gave lines that were as well formed as the lines on slides that were at room temperature.

Optical Microscopy. Optical microscopy was used as a preliminary screening method to characterize the lines. When discussing the line depositions, height is the vertical height of the line up the slide, width is the horizontal distance of the line across the slide, and thickness is the height of the line above the surface of the slide, Figure 1. Figure 2 shows a composite of two optical microscope images that show examples of the vanadium lines. The figure shows that there are three general regions of a slide. The upper region consists of thin lines that have low order. The lower region consists of thick wide lines that converge at the very bottom to make a continuous region. The middle region is the optimal region consisting of thick and discrete lines that have long-term width (the width divided by the height is the largest, Figure 3). Figure 4 shows that TMABr

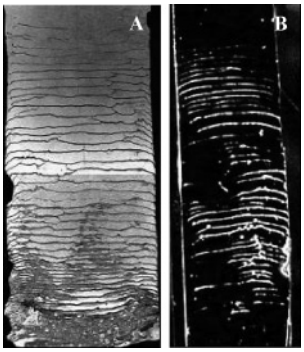

Figure 2. Line formations on silicon wafer: (A) 1×10^{-3} and (B) 1×10^{-4} M TMA−V_2O_5.

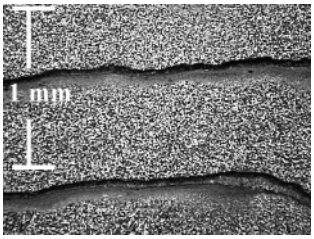

Figure 3. 1×10^{-3} TMA−V_2O_5 line formations on a silicon wafer.

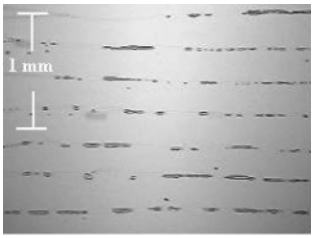

Figure 4. TMABr line formations on a glass slide.

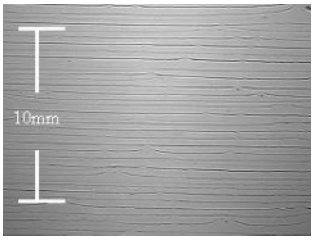

Figure 5. 1×10^{-5} TMA−V_2O_5 line formations on a glass slide.

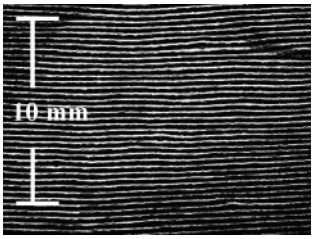

Figure 6. 1×10^{-3} TMA−V_2O_5 line formations on a silicon wafer.

solution forms lines without the presence of the metal. Figure 5 shows lines formed on a glass microscope slide, Figure 6 shows lines formed on a silicon wafer, and Figure 7 shows the lines that form on the backside of a slide.

To evaluate the slides with the optical microscope, a simple scale of −3 to 3 was used to create a bar graph of the variable versus this relative value. The progression of values went from −3 to 3 with the lower score having less ordered formations. These values were determined by looking at the middle 80% of the covered surface.

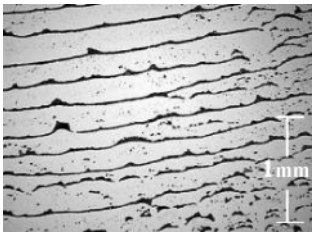

Figure 7. TMA−V_2O_5 line formations on the back of a glass slide.

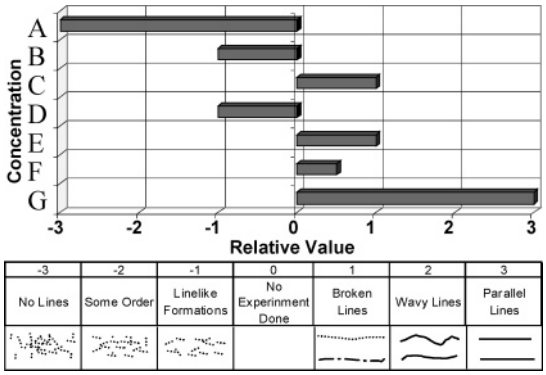

Figure 8. Table of concentration effects and a table of examples of terms used for making the table for a V_2O_5 coated glass slide: (A) 2.0×10^{-2}, (B) 1.0×10^{-2}, (C) 5.0×10^{-4}, (D) 1.0×10^{-4}, (E) 3.3×10^{-5}, (F) 1.0×10^{-5}, and (G) 1.0×10^{-6}.

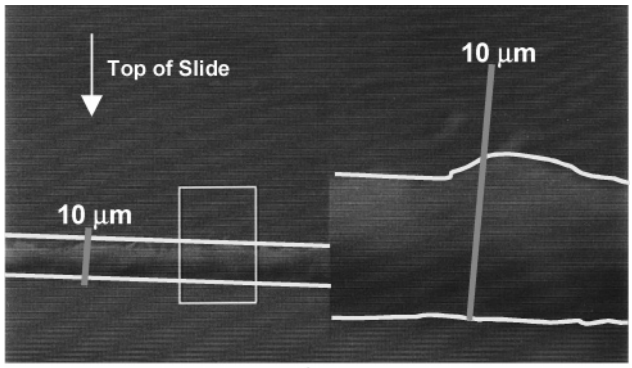

Figure 9. SEM of 1×10^{-4} TMA−V_2O_5 line formations on silica wafer.

Concentration Effects. Concentration played a role in the way the lines formed as Figure 2 shows. Figure 2b shows the same compound at a 10-fold dilution. Lines in the more dilute solution were more separated. A graph of concentration versus the relative value defined above is shown in Figure 8. The bar graph illustrates that as the concentration increased the lines became less discrete and the continuous region increased. This graph is of one set of data, but is typical of the slides evaluated in other trials. In summary, as the concentration of the solution decreased, the lines became more discrete and more parallel, but there was less overall coverage.

Temperature Effects. Temperatures of 180, 120, 100, 85, and 60 °C and room temperature were used. The most uniform lines occurred at 85 °C; the room temperature solution also formed lines that were less parallel.

Scanning Electron Microscopy. A typical SEM micrograph for the lines is presented in Figure 9. Figure 9 shows the scale of a single line (this is an SEM image of the sample in Figure 2B). Line height varied depending on the region of the slide and the section of the line that was studied. Generally speaking, the narrowest lines that could be distinguished were around 10 μm. The average line was on the order of 10 to 30 μm in the

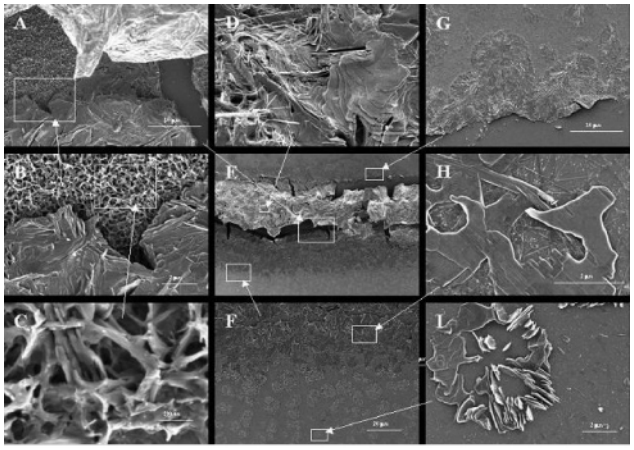

Figure 10. FE SeM of 1×10^{-4} TMA$-V_2O_5$ line formations on silica wafer. (A) An enlargement of panel E showing the substrate in the right-hand side as a channel, the bulk line material at the top, a layered morphology at the bottom left, and a shorter crystal morphology between the bulk material and the layered morphology. (B) An enlargement of panel A showing the shorter crystal morphology at the top and the layered morphology at the bottom. (C) An enlargement of panel B showing the shorter crystal morphology. (D) An enlargement of panel E showing the bulk line morphology. (E) The calcined line of Figure 9. (F) An enlargement of panel E showing the lower line material. (G) An enlargement of panel E showing the upper line material. (H) An enlargement of panel F showing the planar morphology. (I) An enlargement of panel F showing a circular crystalline formation.

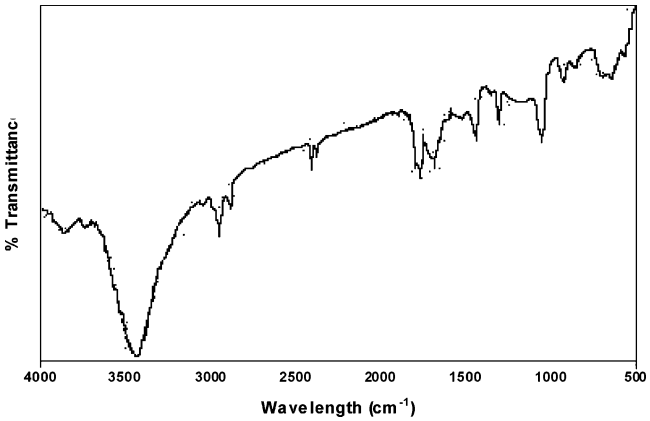

Figure 11. IR spectrum of line material scraped off a slide.

middle region, and lines in the continuous region could be around 100 μm.

The images from the FE-SEM, Figure 10, show that the line material had three different morphologies. There seems to be a porous shorter crystalline material in closest contact to the substrate (Figure 10C). Then there is a less organized more compact material that comprises the major bulk of the line (Figure 10D). Finally, there is a flat crystalline material on the trailing edge (Figure 10H,I). Figure 10E shows that this line segment is cracked. The EDAX experiments done in conjunction with both SEM instruments showed that vanadium is the major component of the lines. The only other element detected was oxygen.

Infrared Spectroscopy. A representative spectrum of an uncalcined sample is shown in Figure 11. Peaks at 3400, 1550, 1050, and 650 to 900 cm^{-1} are indicative of NH stretching, NH bending, C$-$N stretching, and N$-$H rocking modes, respectively. Peaks at 2900, 1350 to 1500, and 625 to 900 are indicative of C$-$H stretching, C$-$H bending, and C$-$H rocking

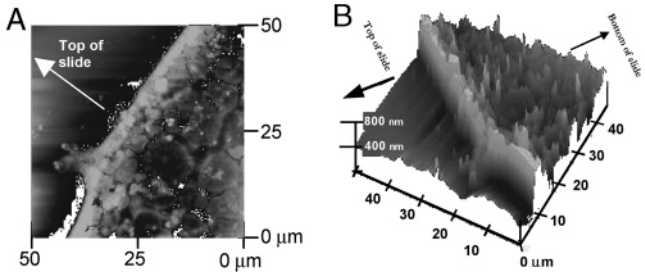

Figure 12. (A) AFM top view of TMA$-V_2O_5$ 1×10^{-4} TMA-V_2O_5 line formations on a glass slide. The lighter the color the more raised the ares. (B) AFM profile view of TMA$-V_2O_5$ 1×10^{-4} TMA$-V_2O_5$ line formations on a glass slide.

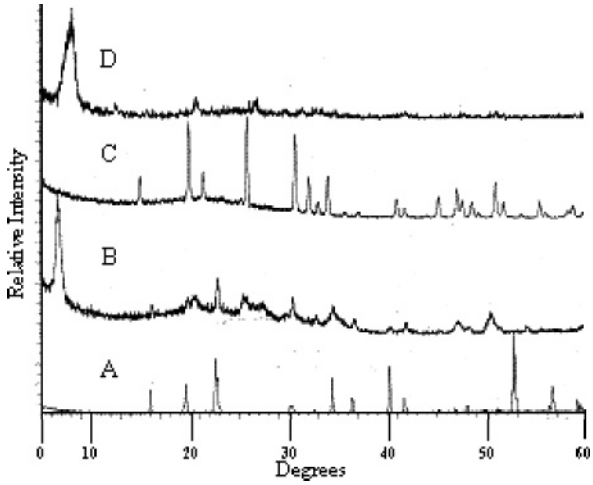

Figure 13. XRD of TMA$-V_2O_5$ 1×10^{-4} TMA$-V_2O_5$ line formations scraped off a glass slide: (A) TMABr, (B) TMA$-V_2O_5$, (C) V_2O_5, and (D) TMA$-V_2O_5$ after calcining.

modes, respectively. Peaks at 1700, 1800, and 2380 are indicative of C═O stretching modes and CO_2, respectively.

Atomic Force Microscopy. AFM data for the line formations show the same line characteristics that were observed with optical microscopy. Figure 12 shows a continuous vanadium oxide line that has a well-defined leading edge and a trailing edge that is made up of smaller particles. Figure 12A shows the top view and Figure 12B shows the profile. The width is around 10 μm with a height of around 0.75 μm.

X-ray Diffraction. Figure 13 shows the XRD pattern for the reactants, TMABr (A) and V_2O_5 (B), and the products, TMA-V_2O_5 (B) and the calcined TMA-V_2O_5 (D). Spectra B and D in Figure 13 both have a peak at around 7 degrees, which is characteristic of a layered vanadium gel. The other smaller peaks are also found in the layered vanadium material. After calcination the peak at 7 °C remains in the diffraction pattern of A and B showing that the structure of the initial material is retained. When B is compared to A and C in Figure 13 there are new peaks that have been formed. This shows that the line material is not a simple mixture of the two starting materials.

Elemental Analysis. Elemental analysis showed that the solid was 9.44% C, 2.89% H, and 2.83% N. This gives mole ratios of 4 C:14 H:1 N, which gives the composition of TMA^+ with two hydrogens left over. The left over hydrogens can be shown to be a part of the vanadium cluster by using a pH vs vanadium molarity diagram.[13] From this diagram, using the corresponding pH and concentration values, it can be shown that the two remaining hydrogens are associated with an individual cluster of the vanadium to form a $V_{10}O_{26}(OH)_2$ cluster. When comparing the amount of vanadium present to the organic content,

further calculations show that there are 2.5 TMA^+ molecules and 3 H^+ atoms associated with each vanadium cluster.

Coating Procedure. The coating results show that the vanadium clusters deposited more material on the PSS coated slides.

Colloidal Silica Procedure. Attempts to increase the amount of suspended vanadium by using colloidal silica produced macroscopic silica crystals, which did not produce line formations.

Discussion

Synthesis. For the vanadium synthesis TMABr was important in the line formation process; the butyl alcohol had no effect on the lines. The reason an alcohol was used in the manganese synthesis was to oxidize the manganese, but the vanadium lines did not seem to require this step. When TMABr was left out of the procedure the lines formed were similar although less regular. The lines formed without TMABr were comparable to the ones that formed on the back of the slides (Figure 7). This difference could have been from the TMABr acting as a templating agent to attach the vanadium to the slide.

From the data gathered, there seems to be no difference in the lines formed on silicon and the glass microscope slides. This is to be expected because both surfaces have exposed surface hydroxyl groups, which would facilitate the line formation process. Materials such as metal, wood, wood pulp materials, and plastics did not work as substitutes, showing the importance of the substrate in the line formation process. These materials might facilitate line growth with proper pretreatment.

It took 4 days for the pH to become constant because of the low solubility of the V_2O_5. The composition determined by elemental analysis is also the predicted composition from the pH measurements.

Concentration. The data show that concentration is an important factor in line formation. Dependence on the availability of the solute is important. With less solute present there is less material to deposit or adsorb onto the substrate. This produces lines that are not as thick and more discrete. As the concentration increases the amount of solute available to deposit or adsorb also increases. This leads to slides that have more deposited material. The thermal energy creates convection currents, which help to support the particles and provide the energy to evaporate the solvent at a rate that facilitates line growth in three dimensions. Too much thermal energy and the precursor materials might not have sufficient time to organize before the solvent evaporates causing the lines to be less ordered. Too little thermal energy and the particles are not mobile enough causing the material to agglomerate at the bottom.

SEM. The different morphologies shown in the FE-SEM images could have physical or chemical origins. The physical explanation could be due to a temperature gradient caused by the heating of the silicon wafer. The chemical effect could be from the interaction of the vanadium clusters with the surface OH− groups of the silica where there is chemical adsorption initially to the surface and then adsorption to the less crystalline underlayer by other vanadium clusters creating a more crystalline layer. The cracking of the line is likely from the shrinking of the material during the calcination process.

Infrared Spectroscopy. The C−H and N−C moieties were expected because the precursor is TMABr, which has C−H bonds and C−N bonds. The possible peaks of C═O, C−C, and C−O are interesting but are quite possible considering the reaction was done in air; alternately, the oxygen may arise from the metal compound. The strong observed peak near 3500 cm^{-1} indicative of N−H is especially interesting. This peak implies that the methyl groups have been replaced leaving the original nitrogen bonded to hydrogen. This could be due to thermal decomposition or the catalytic nature of the vanadium and oxygen in the material. No literature could be found to corroborate this theory.

AFM. The AFM data show a topological representation of the data observed by using the optical microscope. The AFM images show that there is a large initial deposition of material followed by a slow decrease in the amount of material deposited. This phenomenon happens repeatedly until all the solute is consumed or the solvent is completely evaporated. This is different from previous work[5,6] with manganese, which had a symmetric deposition profile of multiple lines on top of each other formed on a continuous film. This discreet line pattern is unique to this research.

X-ray Diffraction. Some general structural information can be gathered from the XRD patterns. The X-ray diffraction patterns of the two precursors (TMABr and V_2O_5), the material scraped off a slide, and the material of a calcined wafer are shown. The material from the lines has a distinctive layered material peak at 7 °C that is not present in any of the two precursors. This peak is caused by the formation of a new-layered vanadium phase and is typical of the vanadium gels. The initial V_2O_5 does not have such a peak, indicating a structural change into a layered vanadium gel. Since a vanadium gel is present, the pH vs concentration curve[21] can be used along with the elemental analysis to predict a structure of $V_{10}O_{26}$-$(OH)_2$, which correlates to the XRD data taken. After calcinations at 500 °C the distinctive peak remained showing some thermal stability.

Elemental Analysis. The elemental analysis data show that there are TMABr components associated with the vanadium material. The organic components could be in the layer structure or attached to the surface. The IR data suggest that the TMA^+ does not stay intact. If this is the case then it is possible that the components are positioned in the layer structure. Whatever the state the organic components are in, they help with charge adjustment to help the vanadium oxide particles better adhere to the substrate.

Coating Procedure. The coating procedure showed that the vanadium clusters preferred the negatively charged PSS layer, indicating that the charge of the clusters is slightly more positive than negative. This also fits in with the proposed mechanism. The results of the coating tests suggest that the TMA^+ may neutralize some of the charge on the clusters. This could be the reason for the better lines with the TMA^+ present. A proper ionic balance, provided by TMA^+, is important for preparation of gel solutions.

Mechanism. The data show that lines are deposited on the glass surfaces. Figure 14 shows a schematic of the formation process as postulated from the data collected. There are two situations to consider. The first situation occurs in a dilute solution or at the top of a more concentrated solution, and the second occurs in a more concentrated solution or at the bottom of a dilute solution. The first step involves the heating of the solution. As the solution temperature is elevated the surface transition zone starts to heat up more due to a lower barrier for escape. This zone would have more molecules moving between the vapor and liquid phase because of the increased kinetic energy of the molecules. The hotter zone would then dissolve more of the solute.

The attraction between the molecules and the substrate increases with a higher concentration of solute present. The

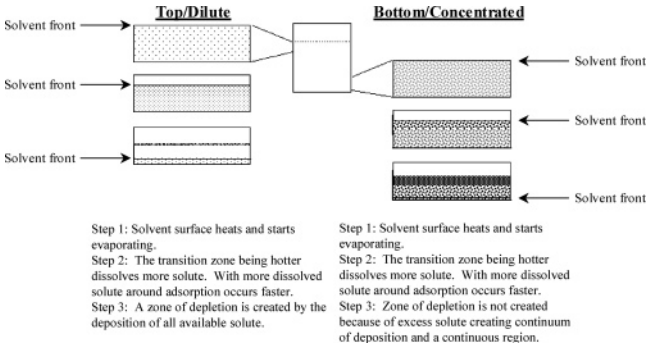

Figure 14. Proposed mechanism for the formation of lines on silicon substrates. Top/Dilute shows what happens at the top of a microscope slide or if the solution is dilute. Bottom/Concentrated shows what might happen at the bottom of a dilute solution or if the solution is concentrated.

particles fall out of solution depositing/adsorbing onto the substrate when the particles can no longer be held in solution. The solute deposits/adsorbs quickly at first causing a well-defined leading edge, and then the process slows down as the solute concentration decreases until all the local solute has been deposited/adsorbed creating a zone of depletion. The well-defined leading edge is evidence that there is no gas-phase adsorption. If material was depositing via the gas phase it would be expected that there would be evidence of deposited material before the leading edge.

In addition, Figure 7 shows the backside of a slide. This side of the slide is angled such that it allows for adsorption only. Figure 7 shows that adsorption along with deposition contribute to the line formation. The difference in line formation in the bottom of a slide or in an initially more concentrated slide was that there seems to be no zone of depletion. There was more solute present, which meant that between the critical deposition points the solute could not be completely depleted. The AFM, SEM, and optical microscopy pictures corroborate this theory. Each of them shows a well-defined leading edge, the trailing edge, and a zone of depletion or a lack of one. Optical microscope images of TMABr only solutions clearly show that lines form. TMA^+ may aid in the adsorption of the metal compound to the substrate. Because of these considerations, it is important to find the optimal temperature to supply enough energy for the self-assembly process to occur at the desired rate.

A mechanism[7] involving initially gravity and then capillary effects has been formulated for the formation of manganese oxide based helices. This manganese oxide helix mechanism could also be applied to the more dilute samples in this work that did not conform to the observed mechanism proposed above. The lines formed on these slides could be from the solution trying to form helices but without the right conditions. Formations such as Figure 2B do not show the characteristic formations of Figure 14. These pictures are similar to the "rib cage" formation steps described in helix formation. The mechanism proposed in this paper dominates at higher concentration conditions while the helix formation mechanism dominates when the concentration is lower. This is important to keep in mind when trying to control the desired product.

Analysis. The lines that are formed on the slides are neither thick nor wide. This has caused problems when using analytical instruments, such as X-ray Photoelectron Spectroscopy, SEM, Transmission Electron Microscopy, and Auger Microscopy, that rely on electron beams for analysis. These instruments are meant to analyze conducting surfaces where charging of the substrate is minimal. With a large percentage of the surface area to be analyzed consisting of the exposed insulating substrate, a charge builds up and the analysis cannot be done. Deposition has been tried on better conducting surfaces such as copper and silicon wafers. The copper did not form lines, instead it made a thin layer on the surface that was not suitable for analysis. The silicon wafers did work well. That was expected because the surface has Si−OH bonds. Depositing line formations on a silica surface may show promise for future uses in electronic circuitry.

Helix formation was attempted. Numerous conditions were investigated and colloidal Si was added to help suspend the particles. Faint, poorly formed, and irregular helices and rings have been observed on the sides of glass tubes when using the vanadium sol−gels.

Conclusions

This work involved the formation of lines from vanadium pentoxide sol−gels. Extensive literature searches have not yielded any line formations synthesized via this route with any metal oxide other than manganese. This work has shown that it is possible to form lines on glass surfaces by immersing a standard microscope slide in the sol−gel. The data that have been collected show some interesting characteristics such as the ability to produce line formations, high reproducibility, dependence on initial concentration, and similar results to previous line work.[5,6] This work has produced spontaneous self-assembled discreet lines with a relatively short and simple procedure. With more work the ability to control inorganic metal solutions could lead to many possible uses such as the assembly of a complex circuit board from a simple metal solution or in the development of television screens.

Acknowledgment. The authors thank the Geosciences and Biosciences Division of the Office of Basic Energy Sciences, Office of Science, U.S. Department of Energy.

References and Notes

(1) Dziembaj, R.; Molenda, M. *J. Power Sources* **2003**, *119*−*121*, 121.

(2) Zhou, Y. K.; Huang, J.; Li, H. L. *Appl. Phys. A: Mater. Sci. Process.* **2003**, *76*, 53.

(3) Liu, J.; Cai, J.; Son, Y. C.; Gao, Q.; Suib, S. L.; Aindow, M. *J. Phys. Chem. B* **2002**, *106*, 9761.

(4) Ching, S.; Roark, J. L.; Duan, N.; Suib, S. L. *Chem. Mater.* **1997**, *9*, 750.

(5) Giraldo, O.; Brock, S. L.; Marquez, M.; Suib, S. L.; Hillhouse, H.; Tsapatsis, M. *Nature* **2000**, *405*, 38.

(6) Giraldo, O.; Marquez, M.; Brock, S. L.; Suib, S. L.; Hillhouse, H.; Tsapatsis, M. *J. Am. Chem. Soc.* **2000**, *122*, 12158.

(7) Veretennikov, I.; Indeikina, A.; Chang, H. C.; Marquez, M.; Suib, S. L.; Giraldo, O. *Langmuir* **2002**, *18* (23), 8792.

(8) Henisch, H. K. *Crystals in Gels and Liesegang Rings*; Cambridge University Press: Cambridge, UK, 1998; pp 6−7.

(9) Samid-Merzel, N.; Lipson, S. G.; Tannhauser, D. S. *Physica A* (*Amsterdam, Neth.*) **1998**, *257*, 413.

(10) Krumeich, F.; Muhr, H. J.; Niederberger, M.; Bieri, F.; Schnyder, B.; Nesper, R. *J. Am. Chem. Soc.* **1999**, *121*, 8324.

(11) Moriarty, P. *Rep. Prog. Phys.* **2001**, *64*, 297.

(12) Chen, K. M.; Jiang, X.; Kimerling, L. C.; Hammond, P. T. *Langmuir* **2000**, *16*, 7825.

(13) Pelletier O.; Davidson P.; Bourgaux C.; Coulon C.; Regnault S.; Livage J. *Langmuir* **2000**, *16*, 5295.

(14) Ditte, A. C. R. *Acad. Sci. Park* **1885**, *101*, 698.

(15) Parvulescu, V. I.; Boghosian, S.; Parvulescu, V.; Jung, S. M.; Grange, P. *J. Catal.* **2003**, *217*, 172.

(16) Chary, K. V. R.; Kishan, G.; Kumar, C. P.; Sagar, G. V.; Niemantsverdriet, J. W. *Appl. Catal. A* **2003**, *245*, 303.

(17) Waku, T.; Argyle, M. D.; Bell, A. T.; Iglesia, E. *Ind. Eng. Chem. Res.* **2003**, *42*, 5462.

(18) Wang, C. B.; Herman, R. G.; Shi, C.; Sun, Q.; Roberts, J. E. *Appl. Catal. A* **2003**, *247*, 321.
(19) Zhai, H. J.; Wang, L. S. *J. Chem. Phys.* **2002**, *117*, 7882.
(20) Hebert, C.; Willinger, M.; Su, D. S.; Pongratz, P.; Schattschneider, P.; Schlogl, R. *Eur. Phys. J. B* **2002**, *28*, 407.
(21) Livage, J. *Chem. Mater.* **1991**, *3*, 578.
(22) Aust, U.; Moritz, T.; Popp, U.; Tomandl, G. *J. Sol-Gel Sci. Technol.* **2003**, *26*, 715.
(23) Lee, T. H.; Kang, E. S.; Bae, B. S. *J. Sol-Gel Sci. Technol.* **2003**, *27*, 23.
(24) Parola, S.; Verdenelli, M.; Sigala, C.; Scharff, J. P.; Velez, K.; Veytizou, C.; Quinson, J. F. *J. Sol-Gel Sci. Technol.* **2003**, *26*, 803.
(25) Ceccato, R.; Carturan, G.; Decker, F.; Artuso, F. *J. Sol-Gel Sci. Technol.* **2003**, *26*, 1071.
(26) Lvov, Y.; Munge, B.; Giraldo, O.; Ichinose, I.; Suib, S. L.; Rusling, J. F. *Langmuir* **2000**, *16*, 8850.